THE JOURNAL OF BIOLOGICAL CHEMISTRY VOL. 284, NO. 36, pp. 24242–24256, September 4, 2009

On the Mechanism of Multiple Lysine Methylation by the Human Mixed Lineage Leukemia Protein-1 (MLL1) Core Complex*[S]◆

Received for publication, April 29, 2009, and in revised form, June 15, 2009 Published, JBC Papers in Press, June 25, 2009, DOI 10.1074/jbc.M109.014498

Anamika Patel, Venkatasubramanian Dharmarajan, Valarie E. Vought, and Michael S. Cosgrove[1]

From the Department of Biology, Syracuse University, Syracuse, New York 13244

Transcription in eukaryotic genomes depends on enzymes that regulate the degree of histone H3 lysine 4 (H3K4) methylation. The mixed lineage leukemia protein-1 (MLL1) is a member of the SET1 family of H3K4 methyltransferases and is frequently rearranged in acute leukemias. Despite sequence comparisons that predict that SET1 family enzymes should only monomethylate their substrates, mono-, di-, and trimethylation of H3K4 has been attributed to SET1 family complexes *in vivo* and *in vitro*. To better understand this paradox, we have biochemically reconstituted and characterized a five-component 200-kDa MLL1 core complex containing human MLL1, WDR5, RbBP5, Ash2L, and DPY-30. We demonstrate that the isolated MLL1 SET domain is a slow monomethyltransferase and that tyrosine 3942 of MLL1 prevents di- and trimethylation of H3K4. In contrast, a complex containing the MLL1 SET domain, WDR5, RbBP5, Ash2L, and DPY-30, displays a marked ~600-fold increase in enzymatic activity but only to the dimethyl form of H3K4. Single turnover kinetic experiments reveal that the reaction leading to H3K4 dimethylation involves the transient accumulation of a monomethylated species, suggesting that the MLL1 core complex uses a non-processive mechanism to catalyze multiple lysine methylation. We have also discovered that the non-SET domain components of the MLL1 core complex possess a previously unrecognized methyltransferase activity that catalyzes H3K4 dimethylation within the MLL1 core complex. Our results suggest that the mechanism of multiple lysine methylation by the MLL1 core complex involves the sequential addition of two methyl groups at two distinct active sites within the complex.

Lysine methylation of histones is an important epigenetic indexing system for transcriptionally active and inactive chromatin domains in eukaryotic genomes (1). Lysine residues can be mono-, di-, or trimethylated at the ϵ-amino group, with each state correlating with a distinct functional outcome (2). For example, trimethylation of histone H3 lysine 4 (H3K4me3) is enriched at the 5′ ends of actively transcribed genes in a wide range of eukaryotes (3, 4) and is thought to regulate transcription through the recruitment of proteins that activate (5–7) or repress transcription (8). In contrast, H3K4 monomethylation (H3K4me1) is enriched in nucleosomes at the 3′-ends of genes (2, 4, 9) or in the distal enhancer sequences of active genes (10). In addition, H3K4 monomethylation in *Saccharomyces cerevisiae* (11–13) and *Chlamydomonas reinhardtii* (14) is associated with gene silencing. These results suggest that distinct strategies have evolved to regulate the degree of H3K4 methylation in eukaryotic genomes. Although numerous histone lysine methyltransferases and demethylases have been identified in recent years (15, 16), relatively little is understood about how the different states of lysine methylation are achieved and regulated.

The majority of histone lysine methyltransferases that have been identified share a conserved SET domain motif, named for its presence in diverse *Drosophila* chromatin regulators: ***SU****(VAR)3–9,* ***E****(z),* and ***Trx*** (17–19). SET domain proteins can be classified into different families based on sequence similarities, substrate specificity, and other structural features and include the SUV39, SET1, SET2, E(z), RIZ, SMYD, and SUV2–20 families (20). It has been suggested that SET1p, the founding member of SET1 class of SET domain proteins, is the sole H3K4 methyltransferase in *S. cerevisiae* (12), and its deletion results in defects in growth, transcriptional silencing, and telomere maintenance (11, 12). In mammals, six SET1 family members have been identified: SET1a and SET1b (21, 22) and four mixed lineage leukemia (MLL)[2] family H3K4 methyltransferases, MLL1, MLL2, MLL3, and MLL4 (23–27). Evidence suggests that the enzymatic activity of SET1 family members is regulated by interaction with a conserved subcomplex of proteins that include WDR5, RbBP5, and Ash2L (28–30). The best characterized mammalian SET1 family member is MLL1 (also known as ALL1, HRX, and Htrx), which has been shown to be important for the maintenance of *HOX* gene expression patterns in hematopoiesis and development (24, 31–34). The C-terminal SET domain is responsible for the H3K4 methylation activity of MLL1, which is thought to be a general mechanism for MLL1-mediated transcriptional regulation (32).

SET domain proteins differ in their ability to utilize mono- and dimethylated lysine side chains as substrates for further methylation, a phenomenon known as product specificity (35). Structure-function studies suggest that product specificity is determined by the presence of a tyrosine or phenylalanine at a key position in the SET domain active site, called the "Phe/Tyr switch" position (36–40). SET domain enzymes with a phen-

* This work was supported in part by research grants from the March of Dimes Birth Defects Foundation (Grant 5-FY06-585), from the Leukemia Research Foundation, a Research Scholar Grant (RSG-09-245-01-DMC) from the American Cancer Society (to M. S. C.), and by funds from Syracuse University.

◆ This article was selected as a Paper of the Week.

[S] The on-line version of this article (available at http://www.jbc.org) contains supplemental Fig. 1.

[1] To whom correspondence should be addressed: Syracuse University, 107 College Place, Syracuse, NY 13244. Tel.: 315-443-2964; Fax: 315-443-2012; E-mail: mscosgro@syr.edu.

[2] The abbreviations used are: MLL, mixed lineage leukemia protein; AdoMet, *S*-adenosyl methionine; MALDI-TOF, matrix-assisted laser desorption/ionization-time of flight.

ylalanine at the switch position, like Dim5 and G9a (40, 41), have larger active site volumes that can accommodate the side chain rotation required for the processive addition of more than one methyl group. In contrast, SET domain enzymes with a tyrosine at the switch position, like SET7/9 and SET8 (39, 42), have a relatively limited active site volume and are predominantly monomethyltransferases. Although mutagenesis experiments have validated the Phe/Tyr switch hypothesis for several SET domain enzymes (40, 43), enzymes from the SET1 family appear to contradict this rule (43). This is because SET1 family enzymes are predicted to monomethylate their substrates based on the presence of a conserved tyrosine at the switch position. However, chromatin immunoprecipitation experiments suggest that SET1 family enzymes are capable of mono-, di-, and trimethylation *in vivo* (2, 9). In addition, a purified MLL1 complex was shown to catalyze mono-, di, and trimethylation of H3 peptides *in vitro* (24). These results suggest that either the product specificity of SET1 family enzymes is established by a mechanism distinct from the Phe/Tyr switch hypothesis or the product specificity of these enzymes is regulated by specific protein-protein interactions in the cell. An understanding of this paradox has been limited by the absence of a well defined system to examine the product specificity of SET1 family enzymes in the presence and absence of interacting proteins.

To better understand how product specificity is regulated in SET1 family enzymes, we have developed an *in vitro* system to identify the molecular mechanisms of H3K4 methylation by the human MLL1 core complex. We previously reported the identification of a minimal MLL1 SET domain fragment that is required for the interaction between the MLL1 and WDR5 components of the MLL1 core complex (44, 45). In this investigation, we used this MLL1 SET domain fragment to reconstitute and characterize the hydrodynamic and kinetic properties of a five-component 200-kDa MLL1 core complex including MLL1, WDR5, RbBP5, Ash2L, and DPY-30. Our results confirm that the isolated MLL1 SET domain is an H3K4 monomethyltransferase, consistent with the predictions of the Phe/Tyr switch hypothesis. In contrast, when the MLL1 SET domain fragment is assembled with a complex containing WDR5, RbBP5, Ash2L, and DPY-30, the rate of lysine methylation is dramatically increased but only to the dimethyl form of H3K4, suggesting that the MLL1 core complex is predominantly a dimethyltransferase. Unexpectedly, we demonstrate that the H3K4 dimethylation activity of the MLL1 core complex is catalyzed by a previously unrecognized methyltransferase activity conferred by the non-SET domain components of the MLL1 core complex. These results suggest that SET1 family complexes have evolved a novel mechanism to precisely regulate the degree of H3K4 methylation in eukaryotes.

EXPERIMENTAL PROCEDURES

Protein Expression and Purification—A human MLL1 construct consisting of residues 3745–3969 (MLL^{3745}) as well as full-length human WDR5, RbBP5, and ASH2L proteins were individually expressed in *Escherichia coli* (Rosetta II, Novagen) and purified as described previously (45). A cDNA clone of the human *dpy-30* gene was obtained from Open Biosystems (clone ID LIFESEQ1240436), PCR-subcloned into the pHis parallel vector (46), and purified by nickel affinity and gel filtration chromatography as described previously (45). As a final step of purification and for buffer exchange, all proteins were passed through a gel filtration column (Superdex 200, GE Healthcare) pre-equilibrated with 20 mM Tris (pH 7.5), 300 mM NaCl, 1 mM tris(2-carboxyethyl)phosphine, and 1 μM $ZnCl_2$.

Analytical Ultracentrifugation—Analytical ultracentrifugation experiments were carried out using a Beckman Coulter ProteomeLabTM XL-A analytical ultracentrifuge equipped with absorbance optics and an eight-hole An-50 Ti analytical rotor. Sedimentation velocity experiments were carried out at 10 °C and 50,000 rpm (200,000 $\times$ *g*) using 3-mm two-sector charcoal-filled Epon centerpieces with quartz windows. Each sample was scanned at 0-min time intervals for 300 scans. Protein samples were run at various concentrations and combinations as described under "Results." Sedimentation boundaries were analyzed by the continuous sedimentation coefficient distribution (c(s)) method using the program SEDFIT (47). Equilibrium dissociation constants for all binary complexes were obtained by globally fitting sedimentation velocity data using the single-site hetero-association model ($A + B \leftrightarrow AB$) of SEDPHAT (48, 49). The program SEDNTERP version 1.09 (50) was used to correct the experimental *s* value to standard conditions at 20 °C in water ($s_{20,w}$) and to calculate the partial specific volume of each protein.

MALDI-TOF Mass Spectrometry Methyltransferase Assays—MALDI-TOF mass spectrometry assays were carried out as described previously (45). Briefly, 6 or 30 μg of MLL^{3745} were mixed with 250 μM *S*-adenosyl methionine (AdoMet) and 10 μM histone H3 peptide consisting of residues 1–20 in a buffer containing 50 mM Tris-Cl, pH 9.0, 200 mM NaCl, 3 mM dithiothreitol, and 5% glycerol. The total reaction volume was 20 μl. To prevent enzyme inactivation over the duration of the experiment, the reactions were incubated at 15 °C for 24 h, and at various time points, aliquots were removed and quenched by the addition of trifluoroacetic acid to 0.5%. The quenched samples were diluted 1:5 with α-cyano-4-hydroxycinnamic acid. MALDI-TOF mass spectrometry was performed on a Bruker AutoFlex mass spectrometer (State University of New York, Oswego, NY) operated in reflectron mode. Final spectra were the average of 100 shots/position at 10 different positions chosen at random on each spot. Duplicate or triplicate measurements were taken at each time point.

[^{3}H]Methyl Transfer Assays—Unmodified histone H3 peptide (residues 1–20), or mono-, di-, and trimethylated H3K4 peptides (residues 1–21) were purchased from Global Peptide and Millipore, respectively. All peptides contained a Gly-Gly linker on the C terminus followed by lysine with biotin on the ϵ-amino group. H3K4 methyltransferase assays were conducted by combining 2 μg of MLL^{3745}-WDR5-RbBP5-Ash2L complex with 250 μM histone H3 peptide and 1 μCi of [^{3}H]methyl-*S*-adenosyl-methionine ([^{3}H]AdoMet, GE Healthcare) in 50 mM Tris, pH 8.5, 200 mM NaCl, 3 mM dithiothreitol, 5 mM $MgCl_2$, and 5% glycerol. The reactions were incubated at 15 °C for 8 h, stopped by the addition of 1$\times$ SDS loading buffer, and separated by SDS-PAGE on a 4–12% gradient gel (Invitrogen). The gel then was soaked in an autoradiography enhancer

solution (ENLIGHTNING, PerkinElmer Life Sciences), dried, and exposed to film at −80 °C for 24 or 48 h.

Pre-steady State Kinetics—Enzymatic reactions were initiated with substrate quantities of enzyme (12 or 60 μM) and were quenched manually at various time points by the addition of 0.5% trifluoroacetic acid. MALDI-TOF mass spectrometry was used to determine the relative distribution of unmodified, mono-, di-, and trimethylated species in each reaction using a procedure similar to that described by Frey and colleagues (51). We note that although MALDI-TOF is generally believed to be a qualitative technique, it has been successfully used in several systems to quantitate reaction intermediates in rapid reaction kinetic experiments with results comparable with other rapid reaction techniques (51, 52). In the present investigation, data were quantitated by determining the percentage of total integrated area for each species and using standard curves to estimate the concentration of each modified form at each time point. Standard curves were constructed by collecting MALDI-TOF spectra on peptide mixtures containing various ratios of synthetic histone H3 peptides that were either unmodified or previously mono- or dimethylated at H3K4. Amino acid analysis was used to determine peptide stock concentrations (Purdue Proteomics Facility). Relative intensity plots of each species in the presence of varying ratios of the other species are linear (supplemental Fig. 1), indicating that ionization and detection of each species is independent of the concentration of the other species. Control experiments indicated that the presence of enzyme did not significantly affect the ionization behavior of the peptides. Single turnover progress curves for the enzyme-catalyzed reactions were fitted to a kinetic model with one or two irreversible consecutive reactions (A→B→C) using Equations 1–3 as described by Fersht (53).

$$[A] = [A]_0 \exp(-k_1 t) \quad \text{(Eq. 1)}$$

$$[B] = \frac{[A]_0 k_1}{k_2 - k_1}[\exp(-k_1 t) - \exp(-k_2 t)] \quad \text{(Eq. 2)}$$

$$[C] = [A]_0\left\{1 + \frac{1}{k_1 - k_2}[k_2 \exp(-k_1 t) - k_1 \exp(-k_2 t)]\right\} \quad \text{(Eq. 3)}$$

where $[A]_0$ is the concentration of the unmodified peptide at time (t) zero. [B] and [C] represent the concentrations of the monomethylated and dimethylated species in single turnover progress curves, respectively. k_1 and k_2 represent the pseudo-first-order rate constants for the conversion of A→B and B→C, respectively. For reactions with two irreversible consecutive steps, the program DynaFit (BioKin, Ltd.) (54) was used to globally fit Equations 1–3 to the data.

RESULTS

Purification and Characterization of Recombinant MLL1 Core Complex Components—Previous co-immunoprecipitation studies suggest that the minimal complex required for di- and trimethylation of H3K4 includes MLL1, WDR5, RbBP5, and Ash2L (28). To begin to test this hypothesis, we individually overexpressed each component in *E. coli* and purified them to homogeneity (Fig. 1*a*). We also similarly purified the human DPY-30 protein, which was recently shown to interact with the Ash2L component of the MLL3 core complex and is conserved in SET1 family complexes ranging from yeast to humans (30). All proteins were full-length human proteins with the exception of human MLL1, for which we used a recombinant fragment containing residues 3745–3969 (MLL^{3745}). This fragment from the extreme C terminus of MLL1 contains the conserved SET and post-SET domains as well as the conserved *Win* or WDR5 interaction motif in the N-SET region of MLL1 (Fig. 1*b*). The MLL1 *Win* motif was previously demonstrated to be required for the interaction between MLL1 and WDR5 (44, 45, 56) and for the assembly and dimethylation activity of the MLL1 core complex (45). Sedimentation velocity analytical ultracentrifugation experiments were used to characterize the hydrodynamic properties of each protein in isolation and to characterize intermolecular interactions within the complex.

Sedimentation velocity profiles for individual proteins were fitted to a distribution of Lamm equation solutions to determine the diffusion-free sedimentation coefficient distributions (c(s)) (47). As shown in Fig. 1*c*, each individual component is monodisperse in solution with experimental s values independent of protein concentration over the concentration range tested (0.1–1.0 mg/ml) (not shown). Experimental and corrected sedimentation coefficients (s and $s_{20,w}$, respectively), frictional coefficients, and experimentally determined and theoretical molecular masses for each individual protein are summarized in Table 1. Comparison of the experimentally determined and theoretical molecular masses indicates that each protein is monomeric in solution with the exception of DPY-30, which sediments as a monodisperse dimer (Table 1).

Hydrodynamic Characterization of Pairwise Interactions within the MLL1 Core Complex—To characterize the interactions between components within the MLL1 core complex, we mixed equimolar amounts of each protein in all possible pairwise combinations and determined sedimentation coefficients using sedimentation velocity analytical ultracentrifugation. The interactions that could be detected using this technique are summarized in Table 2 and Fig. 2 and are briefly discussed below.

MLL^{3745}-WDR5—As we reported previously (45), MLL^{3745} forms a strong 1:1 complex with WDR5 that sediments with an s value of 2.87 (3.1 $s_{20,w}$) and a dissociation constant (K_d) of 120 nM (Fig. 2*b* and Table 2). However, in this investigation, no significant interaction could be detected using this technique when MLL^{3745} was mixed individually with RbBP5, Ash2L, or DPY-30 (not shown).

WDR5-RbBP5—A second direct interaction was observed when WDR5 was mixed with RbBP5 at a 1:1 stoichiometric ratio (Fig. 2*c* and Table 2). These proteins formed a complex with an s value of 2.9 (3.1 $s_{20,w}$) and an experimentally determined molecular mass of 87 kDa (Table 2). This molecular mass is ~9% less than that expected for a complex between WDR5 and RbBP5 (95.7 kDa, Table 2), suggesting that the peak at 2.9 represents an equilibrium mixture between free WDR5 and RbBP5 and the WDR5-RbBP5 complex. Consistent with this hypothesis, dilution of the equimolar mixture resulted in the sedimentation peak shifting to lower s values (Fig. 2*c*), suggesting that the complex dissociates on a relatively rapid time scale when compared with the time scale of sedimentation. The K_d value determined for the WDR5-RbBP5 complex is 2.4 μM with a k_{off} value of 3.5×10^{-4} s^{-1} (Table 2). When WDR5 was mixed with Ash2L or DPY-30 in similar experiments,

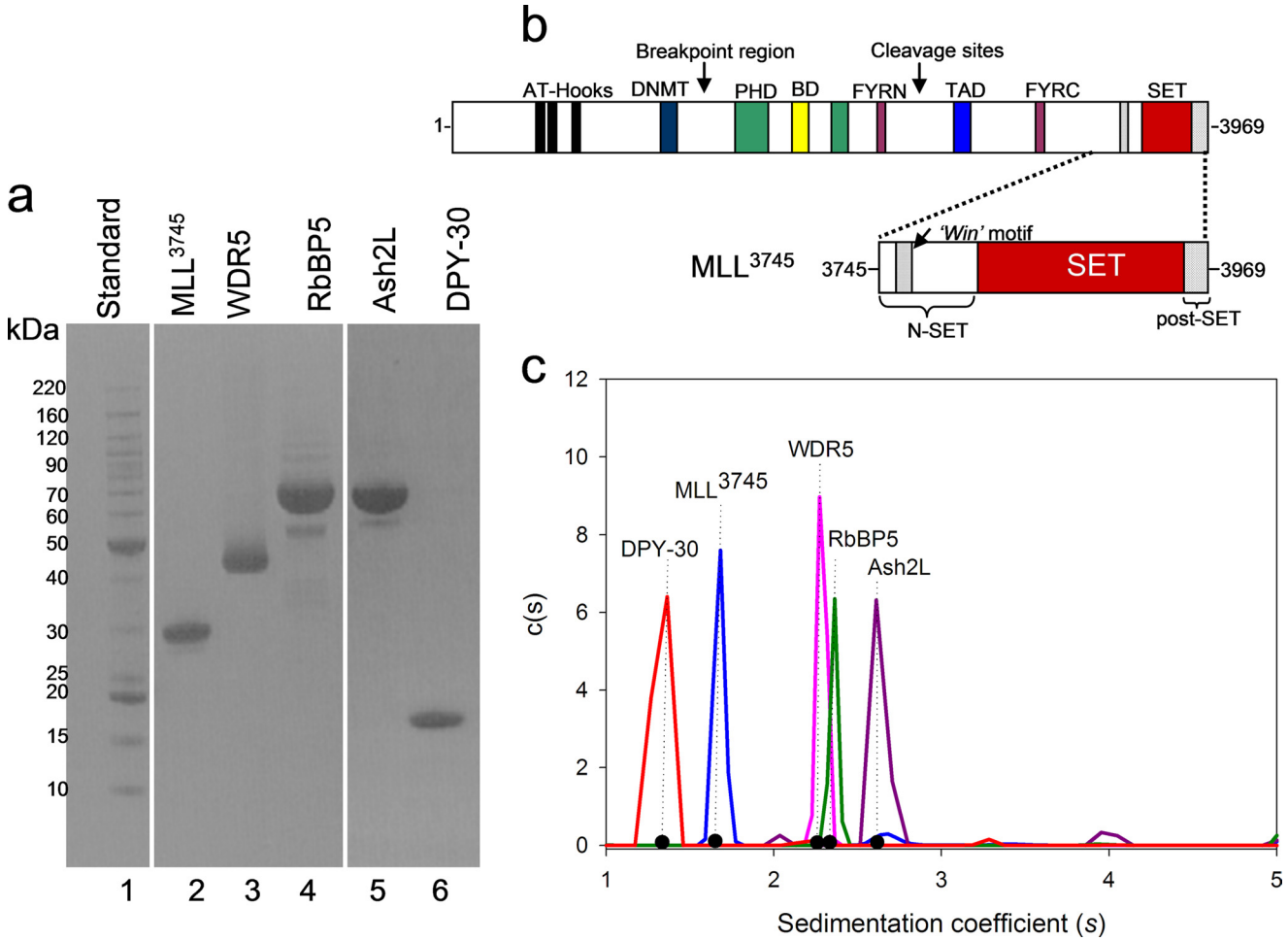

FIGURE 1. **Purification and hydrodynamic characterization of MLL1 core complex components.** *a*, Coomassie Brilliant Blue-stained SDS-PAGE showing the purified MLL1 core complex components. *b*, schematic representation showing the domain architecture of full-length MLL1 and the construct used in this investigation, which consisted of residues 3745–3969 (MLL^{3745}). *c*, diffusion-free sedimentation coefficient distributions (c(s)) derived from sedimentation velocity data of individual MLL1 core complex components: MLL^{3745} (*blue*), WDR5 (*pink*), RbBP5 (*green*), Ash2L (*purple*), and DPY30 (*red*).

TABLE 1

Summary of sedimentation coefficients derived from sedimentation velocity analyses of individual MLL1 core complex components

Protein	s^a	$s_{20,w}{}^b$	f/f_0	Calculated mass	Theoretical mass
				kDa	*kDa*
MLL^{3745}	1.68 ± 0.01	1.76	1.72	26.1	26.1
WDR5	2.28 ± 0.01	2.41	1.51	37.1	36.5
RbBP5	2.37 ± 0.02	2.58	1.97	58.0	59.1
Ash2L	2.64 ± 0.02	2.87	1.83	59.5	60.2
DPY30	1.37 ± 0.01	1.44	1.77	24.0	11.2

[a] Experimental sedimentation coefficient determined at 10 °C (±S.E. from two or three independent experiments).
[b] Standard sedimentation coefficient ($s_{20,w}$) after correcting for water at 20 °C.

TABLE 2

Summary of hydrodynamic parameters and binding constants for pair-wise interactions within the MLL1 core complex

Protein complex	s^a	$s_{20,w}$	K_d $A + B \leftrightarrow AB$	k_{off}, s^{-1}	Calculated mass	Theoretical mass
			μM		*kDa*	*kDa*
MLL^{3745}-WDR5	2.9 ± 0.02	3.1	0.12	1.2×10^{-5}	62.0	62.6
WDR5-RbBP5	2.9 ± 0.02	3.1	2.44	3.5×10^{-4}	87.0	95.7
RbBP5-Ash2L	3.4 ± 0.03	3.7	0.75	4.4×10^{-4}	112.0	119.3
Ash2L-$(DPY30)_2$	3.0 ± 0.01	3.2	0.10	9.7×10^{-6}	83.0	82.6
$(DPY30)_2$	1.4 ± 0.01	1.4	ND[b]	ND[b]	24.0	22.4

[a] Experimental sedimentation coefficient determined at 10 °C (±S.E. from two or three independent experiments).
[b] ND, Not determined. The protein concentration required for determination of the dissociation constant of DPY30 is too low to be detected by the absorbance optical system in sedimentation velocity studies.

no interaction could be observed by sedimentation velocity analytical ultracentrifugation.

RbBP5-Ash2L—When RbBP5 was mixed with an equimolar amount of Ash2L, a complex is formed that sediments with an *s* value of 3.4 (3.7 $s_{20,w}$) (Fig. 2*d* and Table 2). The molecular mass calculated from this sedimentation coefficient was 112 kDa, which is ~6% less than the theoretical mass, suggesting that the complex is less stable on the time scale of sedimentation. Consistent with this hypothesis, there was a significant change in the sedimentation peak when the complex was diluted (Fig. 2*d*). The K_d value determined for the RbBP5-Ash2L complex was 0.75 μM with a k_{off} value of 4.4×10^{-4} s^{-1} (Table 2). No interaction could be detected between RbBP5 and DPY-30.

Ash2L-DPY-30—The last pairwise interaction that could be detected was observed between Ash2L and DPY-30, which forms a stable complex with an *s* value of 3.0 (3.2 $s_{20,w}$) (Fig. 2*e* and Table 2). The experimentally derived molecular mass of this complex was 83 kDa, which is larger than that expected for a 1:1 complex between Ash2L and DPY-30 (71.4 kDa) but within error of that expected for a complex containing one molecule of Ash2L and two molecules of DPY-30 (82.6 kDa). Vary-

a

	MLL^{3745}	WDR5	RbBP5	Ash2L	DPY-30
MLL^{3745}	-	+	-	-	-
WDR5		-	+	-	-
RbBP5			-	+	-
Ash2L				-	+
DPY-30					+

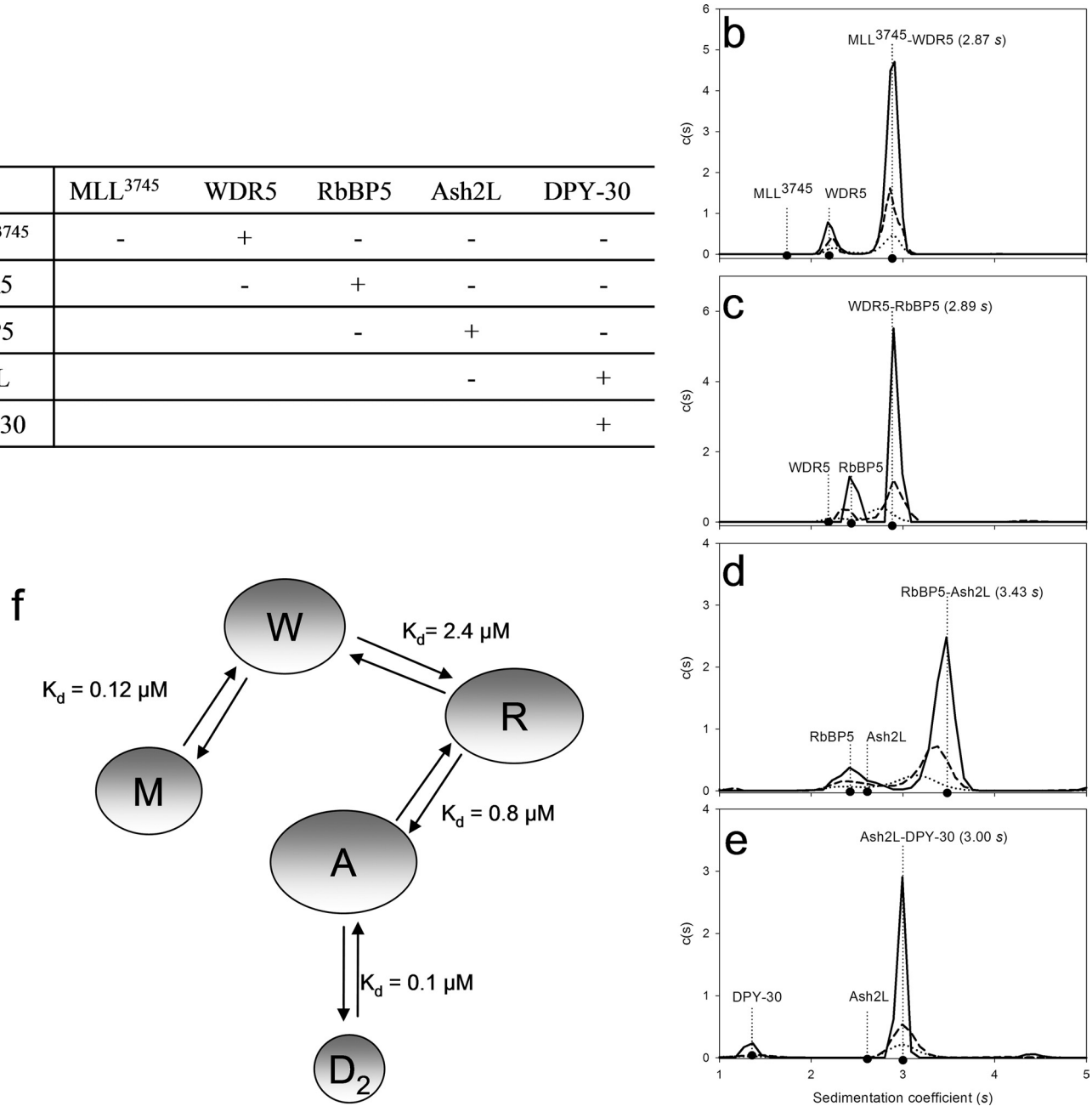

FIGURE 2. **Pairwise interactions within the MLL1 core complex.** *a*, summary of pairwise interactions that could be observed by sedimentation velocity analytical ultracentrifugation. (+) interaction detected; (−) no interaction detected. *b–e*, c(s) distributions of sedimentation velocity data of binary complexes at the following concentrations: 7 μM (*solid black line*), 3.5 μM (*dashed line*), and 1.5 μM (*dotted line*). *b*, MLL^{3745}-WDR5 (reproduced from Ref. 45). *c*, WDR5-RbBP5; *d*, RbBP5-Ash2l; and *e*, Ash2L-DPY-30. *f*, schematic model summarizing the observed pairwise interactions and dissociation constants (K_d) within the MLL1 core complex.

ing the concentration of the complex did not alter the sedimentation peak (Fig. 2*e*), suggesting that the complex is stable on the time scale of sedimentation (48). The K_d determined for the Ash2L-$(DPY\text{-}30)_2$ complex was 100.0 nM with a k_{off} value of 9.7×10^{-6} s^{-1} (Table 2). No direct interaction could be detected between DPY-30 and the other members of the complex. The pairwise interactions observed in these experiments are summarized in Fig. 2*f* and are largely consistent with those reported previously for the MLL1 core complex using co-immunoprecipitation techniques (28) and for the MLL3 and MLL4 complexes using glutathione *S*-transferase pull down experiments (30).

Assembly and Product Specificity of the MLL1 Core Complex—The results from the analysis of pairwise interactions suggest an arrangement for the assembly of MLL1 core complex: MLL1 ↔ WDR5 ↔ RbBP5 ↔ Ash2L ↔ $(DPY\text{-}30)_2$ (Fig. 2*f*). Using this information, we reconstituted the complex in a stepwise manner and compared methylation kinetics and product specificity of MLL^{3745} in the presence and absence of MLL1-interacting proteins. Methylation kinetics were monitored under pre-steady state conditions (substrate quantities of the enzyme) using quantitative MALDI-TOF mass spectrometry (51) to characterize methylation of a histone H3 peptide consisting of residues 1–20. Sedimentation

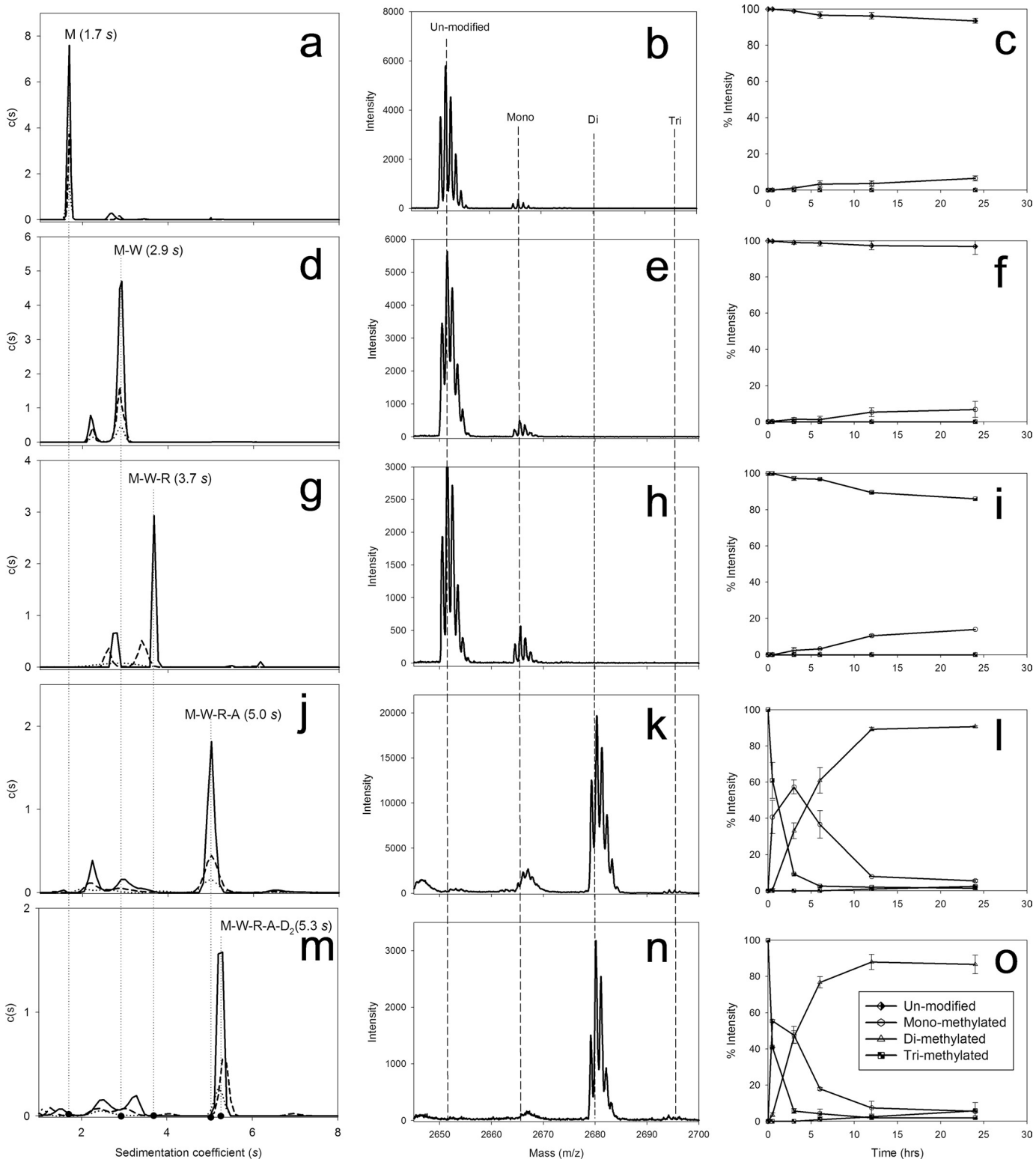

FIGURE 3. **Characterization of the assembly and enzymatic activity of the MLL1 core complex.** The *left column* from *top* to *bottom* shows the c(s) distributions from sedimentation velocity experiments after the addition of each component of the MLL1 core complex starting with: *a*, MLL^{3745} (M); *d*, MLL^{3745}-WDR5 (M-W) (reproduced from Ref. 45). *g*, MLL^{3745}-WDR5-RbBP5 (M-W-R); *j*, MLL^{3745}-WDR5-RbBP5-Ash2L (M-W-R-A); and *m*, MLL^{3745}-WDR5-RbBP5-Ash2L-DPY30 (M-W-R-A-D_2). The *center column* from *top* to *bottom* (*b*, *e*, *h*, *k*, and *n*) shows MALDI-TOF mass spectrometry of enzymatic assays after 24 h. Each spectrum corresponds to the enzymatic activity of the complex in the *c(s) panel* on the *left*. The *third column* from *top* to *bottom* (*c*, *f*, *i*, *l*, and *o*) shows kinetic progression of methylation reactions catalyzed by the corresponding complexes on the *left*. Each time point represents the percentage of total integrated area for each species in MALDI-TOF assays.

velocity analytical ultracentrifugation experiments were carried out under identical protein concentrations to monitor complex assembly.

As described above, MLL^{3745} in the absence of interacting proteins sediments with an *s* value of 1.7 (1.8 $s_{20,w}$) in sedimentation velocity experiments (Fig. 3*a* and Table 3). When the

TABLE 3
Summary of hydrodynamic and kinetic parameters after the addition of each component of the MLL1 core complex

Protein complex	s^a	$s_{20,w}$	f/f_0	Calculated mass	Theoretical mass	$k_1{}^b$
				kDa	*kDa*	h^{-1}
MLL^{3745}	1.7 ± 0.01	1.8	1.7	26.1	26.1	0.003 ± 0.0003
MLL^{3745}-WDR5	2.9 ± 0.02	3.1	1.7	62.0	62.6	0.003 ± 0.0004
MLL^{3745}-WDR5-RbBP5	3.7 ± 0.04	3.9	2.2	110.0	121.7	0.007 ± 0.0004
MLL^{3745}-WDR5-RbBP5-Ash2L	5.0 ± 0.02	5.4	2.0	180.0	179.0	0.93 ± 0.07
MLL^{3745}-WDR5-RbBP5-Ash2L-$(DPY\text{-}30)_2$	5.3 ± 0.01	5.7	2.0	198.0	201.4	1.77 ± 0.11

[a] Experimental sedimentation coefficient determined at 10 °C (±S.E. from two or three independent experiments).
[b] Pseudo-first-order rate constant k_1 (±S.E.) determined from fitting Equation 1 to the disappearance of the relative intensity of the unmodified histone H3 peptide in single turnover progress curves.

enzymatic activity of MLL^{3745} was assayed, only a small amount of the monomethylated form of the histone H3 peptide could be observed after 24 h under these conditions (Fig. 3*b*). To determine the pseudo-first-order rate constant for the reaction catalyzed by MLL^{3745}, we fitted the decrease in the relative intensity of the unmodified peptide over time (Fig. 3*c*) using a model for a single irreversible reaction (A→B) (Equation 1, see "Experimental Procedures"). These data fit with a rate constant of 0.003 ± 0.0003 h^{-1} (Table 3). Together, these data suggest that MLL^{3745} in the absence of interacting proteins is a relatively slow histone H3K4 monomethyltransferase (see below).

We next determined the effect of adding WDR5 to MLL^{3745} on the assembly and enzymatic activity of the MLL1 core complex. When a stoichiometric amount of WDR5 is added to the MLL^{3745} protein, a stable complex is formed (M-W) that sediments with an *s* value of 2.9 ($s_{20,w}$ 3.1) (Fig. 3*d*). However, when the enzymatic activity of the MLL^{3745}-WDR5 complex was assayed, there was no change in the product specificity of MLL (Fig. 3*e*) and no change in the overall rate of the reaction catalyzed by MLL1 (Fig. 3*f* and Table 3). These data indicate that despite forming a stable complex with MLL^{3745}, WDR5 does not significantly increase the enzymatic activity of MLL1.

We next added a stoichiometric amount of RbBP5 to the MLL^{3745}-WDR5 complex (M-W-R) and observed a new sedimentation peak with an *s* value of 3.7 (3.9 $s_{20,w}$) (Fig. 3*g*, *solid line*, and Table 3). The experimentally derived molecular mass of this complex is 110 kDa, which is ~10% less than the theoretical molecular mass of the complex between MLL^{3745}, WDR5, and RbBP5 (Table 3), suggesting that the peak at 3.7 represents an equilibrium mixture of bound and unbound components. Consistent with this hypothesis, dilution of the complex alters the sedimentation coefficient distribution to lower *s* values (Fig. 3*g*, *dashed* and *dotted lines*), suggesting that the complex dissociates relatively rapidly on the time scale of sedimentation. When the histone methylation kinetics for the M-W-R complex were determined, only monomethylation could be observed after 24 h (Fig. 3*h*). However, we observed a small (~2-fold) increase in the overall rate of the reaction catalyzed by the M-W-R complex when compared with that catalyzed by MLL^{3745} alone (Fig. 3*i* and Table 3). Although a direct interaction between RbBP5 and MLL1 could not be detected in our sedimentation velocity assays, our results suggest that RbBP5 may have some interaction with the MLL1 SET domain in the context of the M-W-R complex, which is manifested by a small increase in the enzymatic activity of MLL1. However, our results show that adding WDR5 and RbBP5 to the MLL1 SET domain does not change the product specificity of MLL1.

We next added a stoichiometric amount of Ash2L to the MLL^{3745}-WDR5-RbBP5 complex. Sedimentation velocity experiments showed that Ash2L binds to the complex to form the MLL1 core complex (M-W-R-A) with a sedimentation coefficient of 5.0 *s* (5.4 $s_{20,w}$) (Fig. 3*j* and Table 3). The addition of Ash2L appears to stabilize the whole complex as dilution over a 5-fold concentration range does not alter the position of the sedimentation peak (Fig. 3*j*). Consistent with a stable complex, the molecular mass calculated for this complex was 180 kDa, which is within error similar to the theoretical molecular mass for the four-component complex at 179 kDa with 1:1:1:1 stoichiometry (Table 3). Moreover, the addition of Ash2L to the complex decreases the frictional coefficient (f/f_0) when compared with that of the M-W-R complex (Table 3), suggesting that Ash2L makes the complex more globular.

Strikingly, when Ash2L was added to the MLL^{3745}-WDR5-RbBP5 complex, a considerable change in the methylation kinetics was observed (Fig. 3, *k* and *l*). First, the overall rate of the reaction increased by ~310-fold when compared with that of MLL^{3745} alone (Fig. 3, *k* and *l*, Table 3). Second, almost all of the H3 peptide was converted to the dimethyl form, with only a trace of the trimethyl form visible after 24 h (Fig. 3*k*). Third, intriguingly, methylation kinetics revealed the transient accumulation of the monomethylated peptide that peaked after 3 h of the reaction (Fig. 3*l*). This kinetic behavior suggests that the monomethylated peptide may be released from the active site of the enzyme before rebinding to undergo dimethylation.

To determine whether the addition of DPY-30 could alter the methylation kinetics and product specificity, we added a stoichiometric amount of the DPY-30 dimer to the M-W-R-A complex to form the M-W-R-A-D_2 complex. Sedimentation velocity experiments showed that the sedimentation coefficient of the MLL1 core complex shifts from 5.0 to 5.3 (5.7 $s_{20,w}$) when DPY-30 is added (Fig. 3*m* and Table 3), suggesting that DPY-30 does indeed bind to the MLL1 core complex. The molecular mass determined from this sedimentation coefficient was 198 kDa, which is similar to the expected molecular mass for the interaction of two copies of DPY-30 with the MLL1 core complex (201.4 kDa) (Table 3). When the enzymatic activity of the M-W-R-A-D_2 complex was assayed, the dimethyl form of the histone H3 peptide was observed after 24 h with only a trace of the trimethyl form of H3K4 (Fig. 3*n*). This suggests that the addition of DPY-30 to the MLL1 core complex does not significantly alter product specificity. However, the addition of DPY-30 to the complex increases the overall rate of the reaction by ~2-fold when compared with that of the M-W-R-A complex

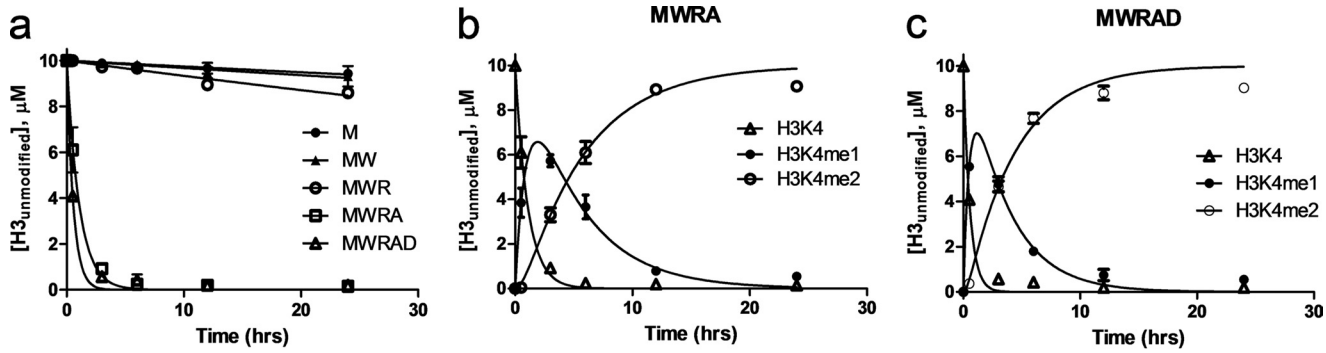

d

Complex	Rate constants, (hr^{-1}) [a]	
	k_1	k_2
MWRA	0.96 ± 0.06	0.21 ± 0.01
MWRAD	1.19 ± 0.10	0.23 ± 0.01

[a] Rate constants (±SEM) derived from global fitting the data to equations 1-3 in experimental procedures.

FIGURE 4. **Determination of rate constants from single turnover progress curves measured by MALDI-TOF mass spectrometry.** *a*, comparison of the overall rates of the reactions catalyzed by MLL^{3745} (*M*) in the presence and absence of MLL1-interacting proteins (W-R-A-D_2). *Solid lines* were derived from fitting the decrease in the relative intensity of the unmodified histone H3 peptide peaks to Equation 1 under "Experimental Procedures." *b*, single turnover progress curves for the reaction catalyzed by the MLL1 core complex (*MWRA*) from MALDI-TOF MS assays. The data for H3K4, H3K4me1, and H3K4me2 species were globally fitted to Equations 1–3 (see "Experimental Procedures") using DynaFit. *Error bars* represent the ±S.E. from duplicate experiments. *c*, single turnover progress curves for the reaction catalyzed by the MLL1 core complex in the presence of DPY30 (*MWRAD*) globally fitted as in *b*. *d*, summary of rate constants (±S.E.) h^{-1} derived from globally fitting experimental data to Equations 1–3 under "Experimental Procedures."

and by ~600-fold when compared with that of the isolated MLL^{3745} SET domain (Table 3).

The differences in the enzymatic activity of MLL1 in the presence and absence of MLL1-interacting proteins are summarized in Fig. 4*a*. As suggested previously (28, 29), the addition of Ash2L to the other components of the MLL1 core complex significantly increases the enzymatic activity of the MLL1 core complex. However, in contrast to previous reports that suggest that Ash2L is required for H3K4 trimethylation (28, 29), we observe only the dimethyl form of H3K4 in our assays, suggesting that the product specificity of the MLL1 core complex is that of a dimethyltransferase. Possible reasons for this difference are presented under "Discussion."

Mechanism of Multiple Lysine Methylation by the MLL1 Core Complex—The kinetic behavior of the MLL1 core complex in the presence and absence of DPY-30 is consistent with a kinetic model with two irreversible consecutive reactions (Reaction 1),

$$\text{H3K4} \xrightarrow{k_1} \text{H3K4me1} \xrightarrow{k_2} \text{H3K4me2}$$

REACTION 1

where the pseudo-first-order rate constant for the first methylation event (k_1) is larger than that of the second methylation event (k_2) (53). Indeed, globally fitting the M-W-R-A profiles using Equations 1–3 (see "Experimental Procedures") reveals that the rate constant for monomethylation (k_1) is 4.6 times larger than that for dimethylation (k_2) (Fig. 4, *b* and *d*). Likewise, globally fitting the data for the reaction catalyzed by the M-W-R-A-D_2 complex results in a k_1 value that is 5.2-fold greater than that of the k_2 value (Fig. 4, *c* and *d*). This kinetic behavior likely accounts for the transient accumulation of the monomethylated peptide during the course of the reaction and suggests that the mechanism of multiple lysine methylation by the MLL1 core complex may be non-processive.

[^{3}H]Methyl Product Specificity Assay—These results suggest that the MLL1 core complex is predominantly a histone H3K4 dimethyltransferase. Because this contrasts with previous reports suggesting that MLL1 core complex catalyzes mono-, di-, and trimethylation (24, 28), we compared the enzymatic activity of the MLL1 core complex among a series of histone H3 peptides that were either unmodified or previously mono-, di-, or trimethylated at H3K4. A more sensitive gel-based assay was used to detect the incorporation of [^{3}H]methyl groups into the peptides using [^{3}H]methyl-*S*-adenosyl methionine ([^{3}H]AdoMet) as the methyl donor. As shown in Fig. 5, the MLL1 core complex possesses robust enzymatic activity with the unmodified and monomethylated H3K4 peptides (Fig. 5, *1anes 1* and *2*, respectively). However, no enzymatic activity could be detected with peptides previously di- or trimethylated at lysine 4 (Fig. 5, *lanes 3* and *4*, respectively). These results confirm that the product specificity of the MLL1 core complex is that of an H3K4 dimethyltransferase.

Tyrosine 3942 of MLL1 Prevents Di- and Trimethylation by the MLL1 SET Domain—The results presented above suggest that the MLL1 SET domain in the absence of interacting proteins is a histone H3K4 monomethyltransferase, which is consistent with the predictions of the Phe/Tyr switch hypothesis (43). To further test this hypothesis, we compared methylation kinetics and product specificity of the wild-type and Y3942F

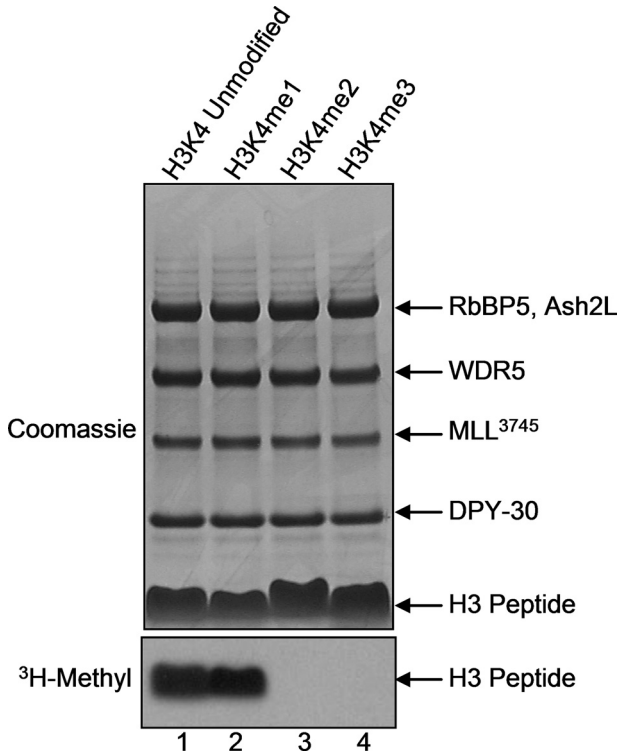

FIGURE 5. **The MLL1 core complex is a histone H3K4 dimethyltransferase.** *Lanes 1–4*, comparison of the enzymatic activity of the MWRAD complex among histone H3 substrates that were unmodified (H3K4, *lane 1*) or previously monomethylated (H3K4me1, *lane 2*); dimethylated (H3K4me2, *lane 3*); or trimethylated (H3K4me3, *lane 4*) at H3K4. The *upper panel* shows a Coomassie Blue-stained SDS-PAGE gel of enzymatic reactions. The *lower panel* shows [^{3}H]methyl incorporation into histone peptides as determined by fluorography.

MLL^{3745} enzymes in the absence of MLL1-interacting proteins. Because tyrosine 3942 of MLL1 occupies the Phe/Tyr switch position (Fig. 6*a*), we predicted that its replacement with phenylalanine would change the product specificity of MLL1 to that of a di- and trimethyltransferase. To accelerate the reaction, we performed the methylation kinetics with a 5-fold higher protein concentration using MALDI-TOF mass spectrometry to follow the kinetic progression of the methylation reactions.

As shown in Fig. 6, *b* and *d*, increasing the protein concentration of the wild-type MLL1 SET domain significantly increases H3K4 monomethylation with a small amount of dimethylation observed after 24 h (Fig. 6*b*). These data are consistent with the hypothesis that the isolated wild type MLL1 SET domain is predominantly a histone H3 monomethyltransferase. However, when tyrosine 3942 of MLL1 was replaced with phenylalanine, mono-, di-, and trimethylated species of the H3 peptide were readily observed after 6 h (Fig. 6*c*). After 24 h, the majority of the peptide was converted into the trimethyl form of histone H3 (Fig. 6*c*), indicating that the Y3942F substitution converts the MLL1 SET domain into a trimethyltransferase. Interestingly, despite the differences in the product specificity of these two enzymes, the first-order rate of the reaction catalyzed by the Y3942F MLL1 SET domain was only slightly increased ($0.086 \pm 0.004\ h^{-1}$) when compared with that of the wild-type MLL1 SET domain ($0.063 \pm 0.005\ h^{-1}$) (Fig. 6, *d* and *e* (see also Fig. 9*a*)), suggesting that the rate-limiting step is similar for both enzymes. In addition, unlike that observed with the MLL1 core complex in which the monomethylated peptide species accumulates to almost 60% of observed peptides in the reaction (Fig. 3, *l* and *o*), the monomethylated peptide species does not accumulate to more than 10% during the course of the reaction catalyzed by the isolated Y3942F MLL^{3745} enzyme (Fig. 6*e*). Instead, the dimethylated peptide accumulates to ~25% before appreciable amounts of the trimethylated peptide are observed. Together, these results suggest that the Y3942F MLL SET domain catalyzes di- and trimethylation of H3K4 using a mechanism that is distinct from that of the MLL1 core complex.

To confirm these results using a different assay, we compared the enzymatic activity of the wild-type and Y3942F MLL^{3745} SET domains using [^{3}H]AdoMet and various histone H3 peptides that were synthesized in the unmodified or lysine 4 mono-, di-, and trimethylated forms. As shown in Fig. 6*f*, wild type MLL^{3745} is predominantly active on the unmodified H3 peptide (Fig. 6*f*, *lane 1*) but is much less active on the monomethylated peptide (Fig. 6*f*, *lane 2*), consistent with the results from the mass spectrometry assays. No activity could be observed with peptides previously di- or trimethylated at lysine 4 (Fig. 6*f*, *lanes 3* and *4*). However, when Tyr-3942 was replaced with phenylalanine, a significant increase in activity was observed with H3 peptides previously mono- and dimethylated at lysine 4 (Fig. 6*f*, *lanes 6* and *7*) when compared with that of the wild-type enzyme. These results indicate that the conserved tyrosine at position 3942 of MLL1 largely limits the intrinsic product specificity of the MLL1 SET domain to that of a monomethyltransferase.

The MLL1 Core Complex Possesses a Previously Unrecognized Methyltransferase Activity That Lacks a Conserved SET Domain—These results raise the question of how the MLL1 core complex can catalyze H3K4 dimethylation when the intrinsic product specificity of the MLL1 SET domain is predominantly that of a monomethyltransferase. A previous investigation suggests that a conformational change in the MLL1 SET domain is required for full activity (58). Alternatively, it is possible that one of the other members of the MLL1 core complex catalyzes the addition of a second methyl group. To distinguish these hypotheses, we assembled the MLL1 core complex with a catalytically inactive variant of the MLL^{3745} SET domain and examined its activity using the [^{3}H]methyl gel assay. Asparagine 3906 of MLL1 is part of a highly conserved NHS motif found in all SET domain enzymes (16) and has been shown to be critical for the enzymatic activity of the SET7/9, SUV39H1, Dim5, and viral SET domain histone methyltransferases (59–63). In addition, in the recent crystal structure of the MLL1 SET domain, Asn-3906 forms a hydrogen bond with the N-terminal methionine moiety of AdoMet (58), suggesting that it is critically important for AdoMet binding. Consistent with this role, we show here that replacement of Asn-3906 of MLL1 with alanine abolishes the histone methyltransferase activity of MLL^{3745} (Fig. 7*a*, *lanes 1* and *2*). This activity loss occurs without a significant change in the ability of MLL^{3745} to assemble into the 5 S MLL1 core complex as measured by sedimentation velocity analytical ultracentrifugation (Fig. 7*b*). Surprisingly, when the N3906A MLL1 SET domain was assembled with the W-R-A-D_2

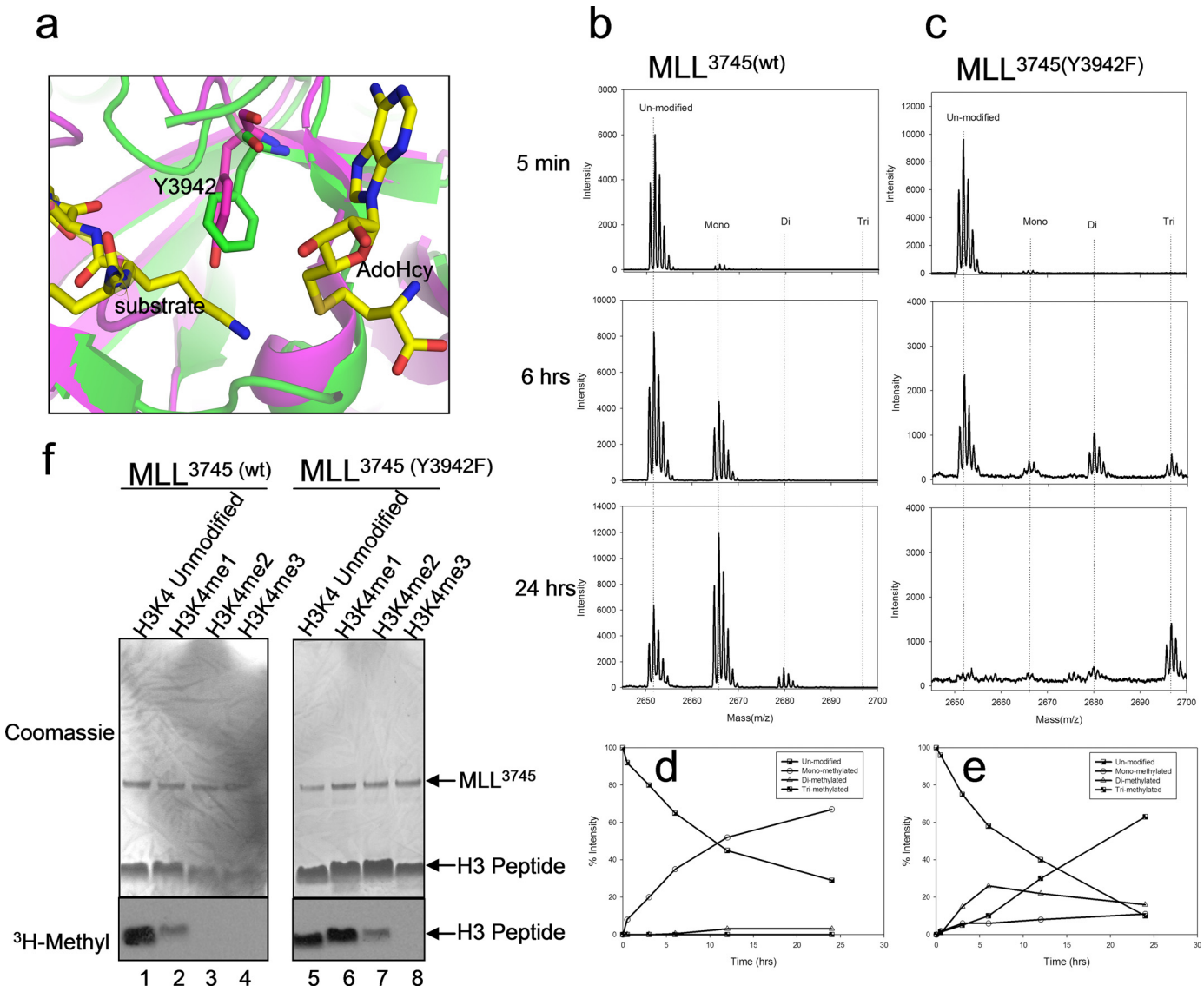

FIGURE 6. **Tyrosine 3942 of MLL1 controls the product specificity of the MLL1 SET domain.** *a*, the Phe/Tyr switch position of the MLL1 (Protein Data Bank (PDB) code: 2W5Z) and Dim5 (PDB code: 1PEG) SET domain active sites are superimposed. MLL1 is shown in *magenta*, and Dim5 is shown in *green*. The position of Tyr-3942 of MLL1 is indicated. The lysine substrate and AdoHcy cofactor are from the Dim5 ternary complex structure and are shown in *yellow*. *b* and *c*, MALDI-TOF mass spectrometry of histone H3 peptide methylation at various time points catalyzed by wild-type MLL^{3745} (MLL$^{3745(wt)}$) (*b*) and Y3942F MLL^{3745} (MLL$^{3745(Y3942F)}$) (*c*). *d* and *e*, kinetic progression of methylation reactions catalyzed by wild-type MLL^{3745} (*d*) and Y3942F MLL^{3745} (*e*). *f*, comparison of the enzymatic activities with different H3K4 substrates between the wild-type (*left panel*) and Y3942F (*right panel*) MLL^{3745} enzymes. The *upper panels* show Coomassie Brilliant Blue-stained gels of methylation reactions, and the *lower panels* show [^{3}H]methyl incorporation into histone peptides as determined by fluorography.

subcomplex, methylation of the histone H3 peptide was restored (Fig. 7*a*, *lane 3*). MALDI-TOF mass spectrometry indicates that the H3 peptide is monomethylated (Fig. 7*c*). These results suggest that one of the non-SET domain components of the MLL1 core complex may be a previously unrecognized histone methyltransferase enzyme. To test this hypothesis, we assembled the complex without MLL1 and tested for histone methyltransferase activity as above. Strikingly, the results show that a complex containing WDR5, RbBP5, Ash2L, and DPY-30, but lacking MLL1, methylates an unmodified histone H3 peptide (residues 1–20) but not H3 peptides previously mono-, di, or trimethylated at H3K4 (Fig. 8*a*). These results indicate that the W-R-A-D$_2$ subcomplex is a previously unrecognized histone methyltransferase that is specific for lysine 4 of histone H3. We note that the complex appears to be required for enzymatic activity as assays with the individual components do not show enzymatic activity on their own (not shown). In addition, because the assays with the individual components lack catalytic activity, contamination with a bacterial methyltransferase activity can be ruled out.

The W-R-A-D$_2$ Subcomplex Catalyzes H3K4 Dimethylation within the MLL1 Core Complex—To determine whether this new activity is required for the H3K4 dimethylation activity of the MLL1 core complex, we assembled the W-R-A-D$_2$ subcomplex with the catalytically inactive MLL1 SET domain and compared the enzymatic activity among histone H3 peptides that were unmodified or previously mono-, di-, or trimethylated at lysine 4. As shown above, although the isolated W-R-A-D$_2$ complex lacks catalytic activity with a peptide previously monomethylated at H3K4 (Fig. 8*a*, *lane 2*), the complex assem-

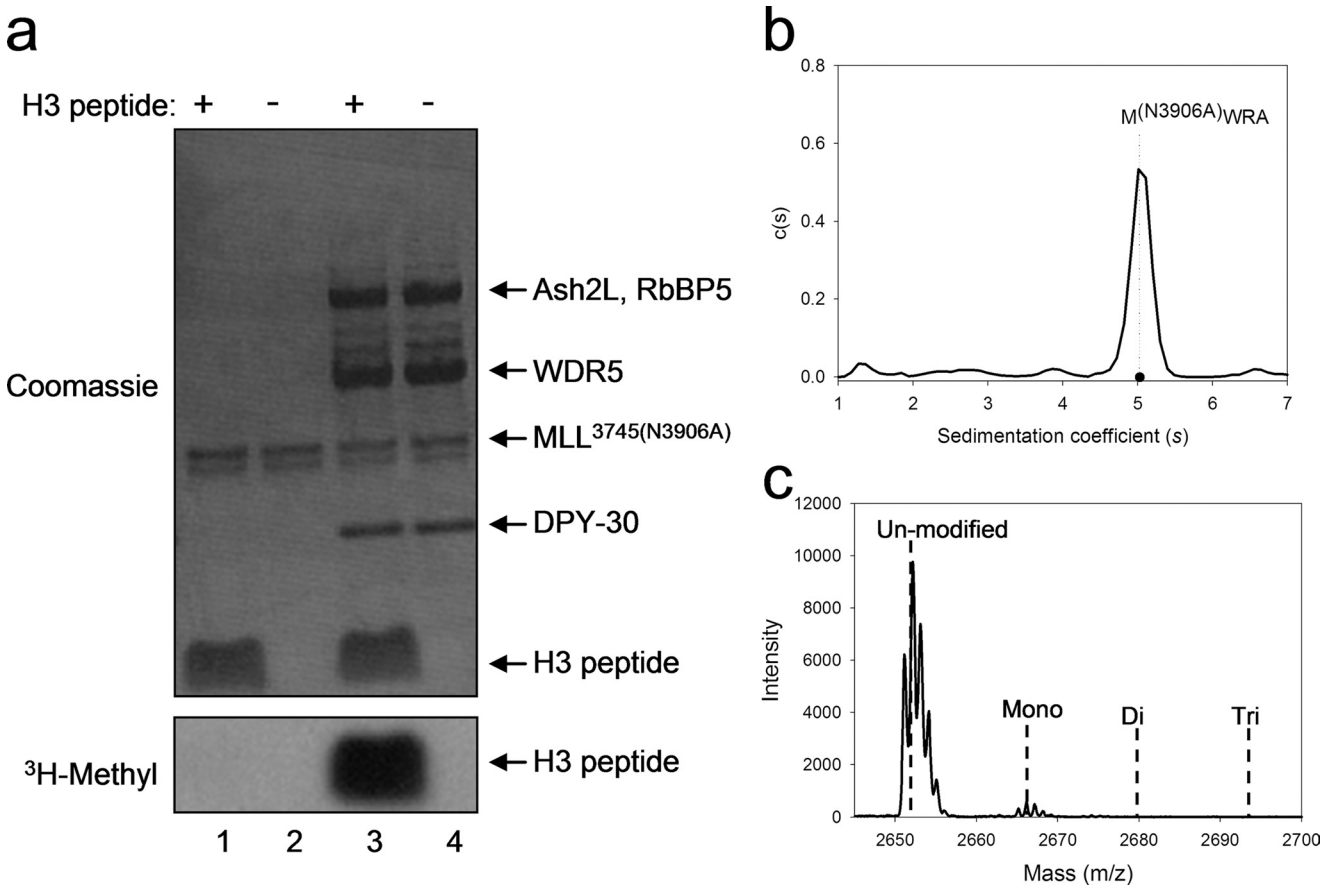

FIGURE 7. **A non-SET domain component of the MLL1 core complex possesses a histone methyltransferase activity.** *a*, enzymatic assays showing that the replacement of asparagine 3906 of MLL1 with alanine ($MLL^{3745(N3906A)}$) abolishes the enzymatic activity of the isolated MLL1 SET domain (*lanes 1* and *2*). *Lanes 3* and *4* show assays with a complex containing $MLL^{3745(N3906A)}$, WDR5, RbBP5, Ash2L, and DPY30. The *upper panel* shows a Coomassie Blue-stained gel of methylation reactions, and the *lower panel* shows the fluorogram of the same gel. *b*, c(s) distribution from sedimentation velocity analytical ultracentrifugation of the MLL1 core complex assembled with stoichiometric amounts of $MLL^{3745(N3906A)}$, WDR5, RbBP5, and Ash2L. *c*, MALDI-TOF mass spectrum of representative methylation reactions catalyzed by the $MLL^{3745(N3906A)}$ SET domain in the presence of WDR5, RbBP5, Ash2L, and DPY30 after 24 h.

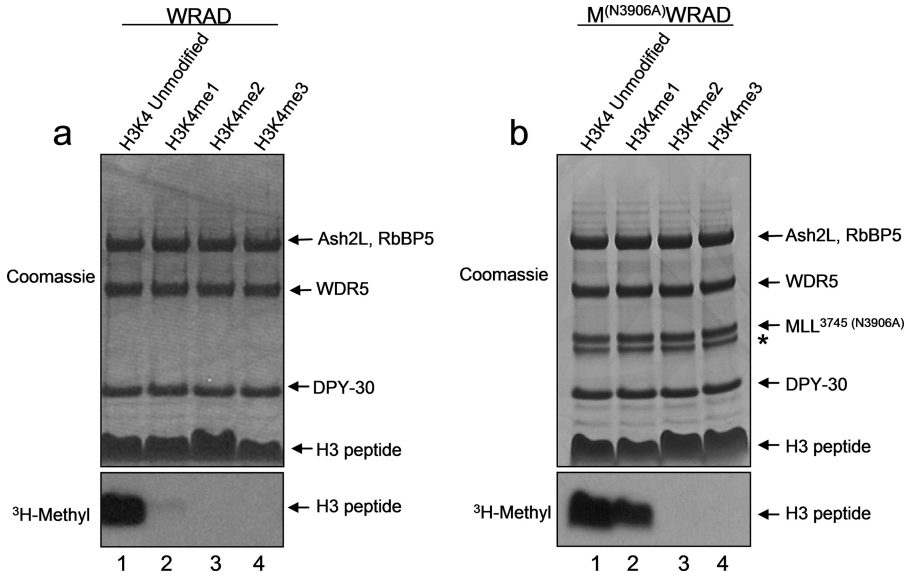

FIGURE 8. **The isolated W-R-A-D_2 subcomplex monomethylates lysine 4 of histone H3 and catalyzes H3K4 dimethylation within the MLL1 core complex.** *a*, comparison of W-R-A-D_2-catalyzed enzymatic activity among histone H3 peptides that were either unmodified (H3K4, *lane 1*) or monomethylated (H3K4me1, *lane 2*); dimethylated (H3K4me2, *lane 3*), or trimethylated (H3K4me3, *lane 4*) at H3K4. The *upper panel* shows Coomassie Blue-stained SDS-PAGE gel, and the *lower panel* shows [^{3}H]methyl incorporation by fluorography. *b*, comparison of the enzymatic activity of the MLL1 core complex assembled with the N3906A MLL1 SET domain among histone H3 peptides as described in *panel a* above. (The protein band indicated by * is partially degraded $MLL^{3745(N3906A)}$.)

bled with the N3906A MLL1 SET domain methylates the monomethylated H3K4 peptide with almost as much efficiency as it methylates the unmodified H3 peptide (Fig. 8*b*, *lanes 1* and *2*). No activity was observed with peptides previously di- or trimethylated at H3K4 (Fig. 8*b*, *lanes 3* and *4*), suggesting that lysine 4 is the residue that is methylated by the mutant complex. Taken together, these results suggest that the W-R-A-D_2 subcomplex is a one-methyl group transfer enzyme that possesses the ability to monomethylate histone H3 on its own or to monomethylate the H3K4me1 substrate when in complex with MLL1.

DISCUSSION

SET1 family enzymes are predicted to monomethylate their substrates on the basis of the presence of a conserved tyrosine residue in

the Phe/Tyr switch position of their active sites. However, mono-, di-, and trimethylation activities have been attributed to SET1 family complexes *in vivo* and *in vitro* (16). An understanding of this paradox is further confounded by conflicting reports on the enzymatic activity of purified MLL1 complexes. For example, Canaani and colleagues (23) reported the isolation of a 29-component mammalian MLL1 supercomplex that is enzymatically active with an unmodified histone H3 peptide but not with a peptide previously dimethylated at H3K4. A similar result was observed with a recombinant MLL1 SET domain fragment containing residues 3745–3969 (23, 32), suggesting that the product specificity of the MLL SET domain is that of either a mono- or dimethyltransferase. In contrast, Roeder and colleagues (24) purified a biochemically distinct mammalian MLL1 complex that is maximally active on a peptide previously dimethylated at H3K4, suggesting that MLL1 is an H3K4 trimethyltransferase. One hypothesis to reconcile these differences is that the product specificity of SET1 family enzymes may be regulated by the unique protein composition of SET1 family complexes. However, our ability to test this hypothesis has been impeded by a lack of information about the intrinsic product specificity of a purified SET1 family SET domain, as well as by a lack of a well defined *in vitro* system to evaluate the role of different complex components on the activity of SET1 family enzymes.

In an effort to identify the minimal complex required for trimethylation by MLL1, Roeder and colleagues (28) developed a baculovirus system to co-express and immunopurify recombinant MLL1 complex components from insect cells. Their results suggest that the minimal complex required for H3K4 trimethylation includes the 180-kDa C-terminal fragment of MLL1 (called MLL-C), WDR5, RbBP5, and Ash2L. However, because the isolated MLL-C fragment lacks catalytic activity on its own, they were unable to assess the intrinsic product specificity of MLL1 in the absence of interacting proteins. In addition, although the co-immunopurification approach has given us valuable information about the assembly and activity of the complex, it suffers from the possibility that unidentified post-translational modifications or co-immunopurified endogenous insect cell proteins could bias the results.

To resolve these issues, we have developed a system for a true biochemical reconstitution of the MLL1 core complex using highly purified recombinant components obtained from over-expression in *E. coli*. This system offers several advantages including the production of large amounts of wild type and mutant proteins for structure-function analyses and the ability to rigorously characterize the biophysical properties of each component individually and within the context of the complex. Although our findings using this system are largely consistent with those reported previously (28, 30), we observe some important differences.

We have identified a minimal enzymatically active MLL1 SET domain fragment that is necessary and sufficient for the reconstitution of the MLL1 core complex *in vitro*. Using this fragment, we have determined the intrinsic product specificity of the MLL1 SET domain in the absence of interacting proteins. Using two different enzymatic assays, we show that the MLL1 SET domain is predominantly an H3K4-specific monomethyltransferase, which is consistent with the predictions of the Phe/Tyr switch hypothesis. This result is further confirmed with the Y3942F substitution in the MLL SET domain, which changes the product specificity of the MLL1 SET domain to that of a trimethyltransferase. Together, these results indicate that the conserved tyrosine at position 3942 of MLL1 largely limits the product specificity of the MLL1 SET domain to that of an H3K4-specific monomethyltransferase.

This MLL1 SET domain product specificity may explain why mutations or deletions that affect the assembly of the MLL1 core complex retain H3K4 monomethylation activity despite significantly losing H3K4 di- and trimethylation activity. For example, substitution of the conserved arginine 3765 of the MLL1 *Win* motif prevents the association of MLL1 with the W-R-A subcomplex, resulting in the loss of the H3K4 dimethylation but not monomethylation activity of the MLL1 core complex (45). A similar result is observed if enzymatic assays are conducted in the absence of WDR5 or in the presence of an MLL1 *Win* motif peptide that competes for the interaction of MLL1 with the W-R-A subcomplex (45). Likewise, insect cell immunoprecipitated MLL1 complexes lacking RbBP5 or Ash2L retain comparable H3K4 monomethylation activity levels but have reduced H3K4 di- and trimethylation levels (28). A similar result is observed upon deletion of the Cps60 (Bre2) (Ash2L homolog) component of the homologous budding yeast SET1 family complex called COMPASS (13).

These results raise the question of how MLL1 can catalyze mono-, di-, and trimethylation of H3K4 *in vivo* when the intrinsic structural properties of the MLL1 SET domain are designed for the addition of predominantly one methyl group. One hypothesis is that proteins that interact with the MLL SET domain may alter the conformation of Tyr-3942 in the SET domain active site, thus allowing di- and trimethylation of H3K4. This hypothesis predicts that the MLL1 core complex will catalyze mono-, di-, and trimethylation with methylation kinetics similar to that observed with the isolated Y3942F MLL1 SET domain. However, the kinetic behavior we observe with the assembled complex is significantly different from that predicted by the conformational change hypothesis, suggesting that the mechanism is distinct. First, despite readily catalyzing mono-, di-, and trimethylation of H3 peptides *in vitro*, the rate constant for the reaction catalyzed by the Y3942F enzyme is only slightly increased when compared with that of the wild-type enzyme (Fig. 9*a*), indicating that both enzymes use a similar rate-limiting step. In contrast, the rate constant for the reaction catalyzed by the M-W-R-A-D_2 complex increases ~600-fold when compared with that of MLL^{3745} alone (Fig. 9*b*), suggesting either that the complex significantly accelerates the rate-limiting step of the reaction or that it uses a different rate-limiting step to catalyze each methylation event. Second, in contrast to that observed with the Y3942F SET domain, the reaction catalyzed by the MLL1 core complex results in a greater transient accumulation of the monomethylated peptide during the course of the reaction (compare Fig. 3*l* and Fig. 6*e*), suggesting that it may be released from the active site before dimethylation occurs. This kinetic behavior is consistent with that expected for a distributive rather than processive mechanism (64). Third, in contrast to the trimethylation activity

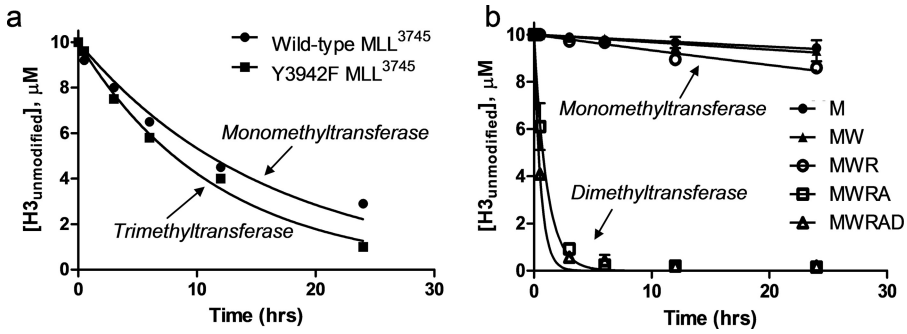

FIGURE 9. **The mechanism of multiple lysine methylation by the MLL1 core complex is distinct from that of the Y3942F MLL1 SET domain.** *a*, comparison of reaction progress curves for the decrease in the relative intensity of unmodified histone H3 peptides catalyzed by the isolated wild-type and Y3942F MLL^{3745} SET domains as determined by MALDI-TOF mass spectrometry. The product specificity of each enzyme is indicated with an *arrow*. *b*, comparison of wild-type MLL^{3745}-catalyzed reaction progress curves for unmodified H3K4 peptides in the presence and absence of MLL1-interacting proteins as determined by MALDI-TOF mass spectrometry.

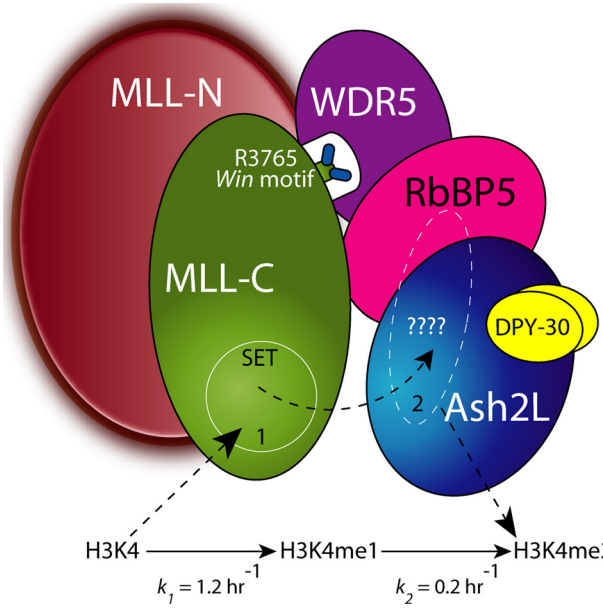

FIGURE 10. **Proposed model for the mechanism of multiple lysine methylation by the MLL1 core complex.** In this model, the MLL1 SET domain catalyzes monomethylation of histone H3 at site 1, which is followed by transfer of the monomethylated peptide to a second active site on the W-R-A-D$_2$ subcomplex (*site 2*, *white dashed oval*), which then catalyzes dimethylation of histone H3. The *white question marks* in *site 2* denote that fact that the catalytic motif of the W-R-A-D$_2$ subcomplex is unknown. The rate constants are derived from the fitting of the data to this model (Fig. 4). Also shown is the interaction between WDR5 and Arg-3765 of the MLL1 Win motif, which was previously shown to be required for the assembly and dimethylation activity of the MLL1 core complex (45).

observed with the Y3942F SET domain, the final product of the reaction catalyzed by the MLL1 core complex is the dimethyl form of H3K4, with little evidence for H3K4 trimethylation under these conditions. Together, these results suggest that the mechanism of multiple lysine methylation by the MLL1 core complex is distinct from that of the isolated Y3942F MLL1 SET domain.

An alternative hypothesis for multiple lysine methylation could be that each methyl group is added by a distinct methyltransferase domain. This hypothesis is consistent with the observed product specificity of the isolated MLL1 SET domain and the observed methylation kinetics for the MLL1 core complex. Our discovery that a novel enzymatic activity catalyzes dimethylation of H3K4 within the MLL1 core complex provides convincing evidence for this type of mechanism. We show for the first time that a complex consisting of WDR5, RbBP5, Ash2L, and DPY-30, but lacking MLL1, possesses a novel histone methyltransferase activity. Importantly, each component lacks catalytic activity when assayed individually, suggesting that the complex is required for functional activity. This complex requirement may explain why this activity has not been observed previously. This discovery is significant in that the components of the W-R-A-D$_2$ complex do not contain a SET (16) or DOT1-like histone methyltransferase fold (57), indicating that it is a novel histone methyltransferase. Because all the components of the W-R-A-D$_2$ complex are required for enzymatic activity, the identity of the catalytic motif is unknown, and the active site could be shared between subunits. Future structure-function studies will be required to elucidate the molecular mechanisms of this new histone methyltransferase.

The observation that the isolated W-R-A-D$_2$ complex is active only with the unmodified H3 peptide suggests that it is an H3K4-specific monomethyltransferase. However, when assembled in a complex with a catalytically inactive MLL1 SET domain, the W-R-A-D$_2$ subcomplex acquires the ability to methylate a peptide previously monomethylated at H3K4. This result indicates that something present only within the holo-complex allows for dimethylation by the W-R-A-D$_2$ subcomplex. Possibilities to explain this altered specificity include an MLL1 SET domain-dependent conformational change in the W-R-A-D$_2$ active site that allows the H3K4me1 peptide to be a substrate. Alternatively, it is possible that the monomethylated peptide is activated for further methylation by an unknown amino acid residue serving as a general base, a residue that is correctly positioned only within the holo-complex. That the holo-complex is required for H3K4 dimethylation may explain why mutations that disrupt the interaction between MLL1 and the W-R-A-D$_2$ subcomplex abolish H3K4 dimethylation but not the monomethylation activity of the MLL1 core complex (45).

On the basis of these data, we propose a new model for the mechanism of multiple lysine methylation by the MLL1 core complex (Fig. 10). Because of the intrinsic product specificity of the MLL1 SET domain and the fact that it possesses a greater methylation activity with the unmodified histone H3 substrate when compared with that of the isolated W-R-A-D$_2$ subcomplex (not shown), we propose that the MLL1 SET domain component of the MLL1 core complex catalyzes the first methylation reaction at a rate that is reflected by the pseudo-first-order rate constant (k_1) in Fig. 10. We suggest that the monomethylated peptide is then released from the MLL1 SET domain active site, where it then binds to a separate active site on the W-R-A-D$_2$ subcomplex to undergo dimethylation. This model is sup-

ported by the observation of the transient accumulation of a monomethylated peptide in single turnover progress curves, which would not be expected if the histone substrate remained bound in a single site during both methylation events. We suggest that the W-R-A-D_2 subcomplex then catalyzes the addition of the second methyl group at a rate that may be represented by the pseudo-first-order rate constant (k_2) (Fig. 10). The fact that the rate constant for the addition of the first methyl group is 5–6-fold greater than that of the second methyl group may be consistent with the idea that two different enzymes, each with their own rate-limiting steps, catalyze each methylation event at distinct sites in the complex. However, it is also possible that k_2 is limited by the transfer of peptide from one active site to the other. Further studies will be required to distinguish these hypotheses.

Lastly, the fact that trimethylation is not observed in our assays is in contrast to that previously reported with the insect cell immunopurified MLL1 core complex (28). Possible reasons for this discrepancy could be that an additional unidentified component co-purifies with the insect cell-derived complex or that a posttranslational modification derived from insect cell expression may be required for H3K4 trimethylation. However, it is also possible that the discrepancy is due to differences in the assays used to determine the degree of H3K4 methylation in different studies. In the investigation by Dou *et al.* (28), methylation state-specific antibodies were used to assess the degree of H3K4 methylation by the insect cell-derived MLL1 core complex. Using this assay, it is difficult to distinguish *bona fide* trimethylation of H3K4 from antibody cross-reactivity with the dimethyl form of H3K4. Indeed, significant cross-reactivity of α-H3K4me3 antibodies with H3K4me2 epitopes has been documented (see supplemental Fig. 1*d* in Ref. 55). Future studies that distinguish among these possibilities will be required to understand how H3K4 trimethylation is achieved and regulated in the cell.

In summary, using a new system to biochemically reconstitute the MLL1 core complex, we have established that the intrinsic product specificity of the MLL1 SET domain is predominantly that of a slow monomethyltransferase and that the product specificity of the MLL1 core complex is that of a relatively fast dimethyltransferase. In contrast to expectations, kinetic and biochemical experiments suggest that the mechanism of multiple lysine methylation by the MLL1 core complex is distinct from that predicted by a conformational change in the MLL1 SET domain active site. Motivated to understand this behavior, we have uncovered a previously unrecognized histone methyltransferase activity conferred by the WDR5, RbBP5, Ash2L, and DPY-30 subcomplex, all components lacking a recognizable histone methyltransferase fold. We provide evidence suggesting that the enzymatic activity of this complex is required for the H3K4 dimethylation activity of the MLL1 core complex. Based on this information, we propose that the mechanism of multiple lysine methylation by the MLL1 core complex involves two distinct active sites, each catalyzing the addition of one methyl group. We suggest that this mechanism provides for an exquisite level of control of the degree of H3K4 methylation in eukaryotic genomes.

Acknowledgments—We thank Tom Starmer (Syracuse University) for help with SAS (Statistical Analysis Software), Petr Kuzmic (BioKin Ltd.) for help with DynaFit, and Bruce Hudson (Syracuse University) for helpful discussions. We thank Anthony Oulette and Kestas Bendinskas for training and access to the MALDI-TOF mass spectrometer at the State University of New York (SUNY) Oswego. We thank Gillian Kupakuwana (Syracuse University) for making the N3906A MLL1 SET domain substitution.

REFERENCES

1. Litt, M. D., Simpson, M., Gaszner, M., Allis, C. D., and Felsenfeld, G. (2001) *Science* **293,** 2453–2455
2. Santos-Rosa, H., Schneider, R., Bannister, A. J., Sherriff, J., Bernstein, B. E., Emre, N. C., Schreiber, S. L., Mellor, J., and Kouzarides, T. (2002) *Nature* **419,** 407–411
3. Liu, C. L., Kaplan, T., Kim, M., Buratowski, S., Schreiber, S. L., Friedman, N., and Rando, O. J. (2005) *PLoS Biol.* **3,** e328
4. Pokholok, D. K., Harbison, C. T., Levine, S., Cole, M., Hannett, N. M., Lee, T. I., Bell, G. W., Walker, K., Rolfe, P. A., Herbolsheimer, E., Zeitlinger, J., Lewitter, F., Gifford, D. K., and Young, R. A. (2005) *Cell* **122,** 517–527
5. Wysocka, J., Swigut, T., Xiao, H., Milne, T. A., Kwon, S. Y., Landry, J., Kauer, M., Tackett, A. J., Chait, B. T., Badenhorst, P., Wu, C., and Allis, C. D. (2006) *Nature* **442,** 86–90
6. Santos-Rosa, H., Schneider, R., Bernstein, B. E., Karabetsou, N., Morillon, A., Weise, C., Schreiber, S. L., Mellor, J., and Kouzarides, T. (2003) *Mol. Cell* **12,** 1325–1332
7. Pray-Grant, M. G., Daniel, J. A., Schieltz, D., Yates, J. R., 3rd, and Grant, P. A. (2005) *Nature* **433,** 434–438
8. Shi, X., Hong, T., Walter, K. L., Ewalt, M., Michishita, E., Hung, T., Carney, D., Peña, P., Lan, F., Kaadige, M. R., Lacoste, N., Cayrou, C., Davrazou, F., Saha, A., Cairns, B. R., Ayer, D. E., Kutateladze, T. G., Shi, Y., Côté, J., Chua, K. F., and Gozani, O. (2006) *Nature* **442,** 96–99
9. Ng, H. H., Robert, F., Young, R. A., and Struhl, K. (2003) *Mol. Cell* **11,** 709–719
10. Heintzman, N. D., Stuart, R. K., Hon, G., Fu, Y., Ching, C. W., Hawkins, R. D., Barrera, L. O., Van Calcar, S., Qu, C., Ching, K. A., Wang, W., Weng, Z., Green, R. D., Crawford, G. E., and Ren, B. (2007) *Nat. Genet.* **39,** 311–318
11. Nislow, C., Ray, E., and Pillus, L. (1997) *Mol. Biol. Cell* **8,** 2421–2436
12. Briggs, S. D., Bryk, M., Strahl, B. D., Cheung, W. L., Davie, J. K., Dent, S. Y., Winston, F., and Allis, C. D. (2001) *Genes Dev.* **15,** 3286–3295
13. Schneider, J., Wood, A., Lee, J. S., Schuster, R., Dueker, J., Maguire, C., Swanson, S. K., Florens, L., Washburn, M. P., and Shilatifard, A. (2005) *Mol. Cell* **19,** 849–856
14. van Dijk, K., Marley, K. E., Jeong, B. R., Xu, J., Hesson, J., Cerny, R. L., Waterborg, J. H., and Cerutti, H. (2005) *Plant Cell* **17,** 2439–2453
15. Agger, K., Christensen, J., Cloos, P. A., and Helin, K. (2008) *Curr. Opin. Genet. Dev.* **18,** 159–168
16. Dillon, S. C., Zhang, X., Trievel, R. C., and Cheng, X. (2005) *Genome Biol* **6,** 227
17. Jones, R. S., and Gelbart, W. M. (1993) *Mol. Cell. Biol.* **13,** 6357–6366
18. Stassen, M. J., Bailey, D., Nelson, S., Chinwalla, V., and Harte, P. J. (1995) *Mech. Dev.* **52,** 209–223
19. Tschiersch, B., Hofmann, A., Krauss, V., Dorn, R., Korge, G., and Reuter, G. (1994) *EMBO J.* **13,** 3822–3831
20. Kouzarides, T. (2002) *Curr. Opin. Genet. Dev.* **12,** 198–209
21. Lee, J. H., and Skalnik, D. G. (2005) *J. Biol. Chem.* **280,** 41725–41731
22. Lee, J. H., Tate, C. M., You, J. S., and Skalnik, D. G. (2007) *J. Biol. Chem.* **282,** 13419–13428
23. Nakamura, T., Mori, T., Tada, S., Krajewski, W., Rozovskaia, T., Wassell, R., Dubois, G., Mazo, A., Croce, C. M., and Canaani, E. (2002) *Mol. Cell* **10,** 1119–1128

24. Dou, Y., Milne, T. A., Tackett, A. J., Smith, E. R., Fukuda, A., Wysocka, J., Allis, C. D., Chait, B. T., Hess, J. L., and Roeder, R. G. (2005) *Cell* **121,** 873–885
25. Hughes, C. M., Rozenblatt-Rosen, O., Milne, T. A., Copeland, T. D., Levine, S. S., Lee, J. C., Hayes, D. N., Shanmugam, K. S., Bhattacharjee, A., Biondi, C. A., Kay, G. F., Hayward, N. K., Hess, J. L., and Meyerson, M. (2004) *Mol. Cell* **13,** 587–597
26. Goo, Y. H., Sohn, Y. C., Kim, D. H., Kim, S. W., Kang, M. J., Jung, D. J., Kwak, E., Barlev, N. A., Berger, S. L., Chow, V. T., Roeder, R. G., Azorsa, D. O., Meltzer, P. S., Suh, P. G., Song, E. J., Lee, K. J., Lee, Y. C., and Lee, J. W. (2003) *Mol. Cell. Biol.* **23,** 140–149
27. Wysocka, J., Myers, M. P., Laherty, C. D., Eisenman, R. N., and Herr, W. (2003) *Genes Dev.* **17,** 896–911
28. Dou, Y., Milne, T. A., Ruthenburg, A. J., Lee, S., Lee, J. W., Verdine, G. L., Allis, C. D., and Roeder, R. G. (2006) *Nat. Struct. Mol. Biol.* **13,** 713–719
29. Steward, M. M., Lee, J. S., O'Donovan, A., Wyatt, M., Bernstein, B. E., and Shilatifard, A. (2006) *Nat. Struct. Mol. Biol.* **13,** 852–854
30. Cho, Y. W., Hong, T., Hong, S., Guo, H., Yu, H., Kim, D., Guszczynski, T., Dressler, G. R., Copeland, T. D., Kalkum, M., and Ge, K. (2007) *J. Biol. Chem.* **282,** 20395–20406
31. Milne, T. A., Dou, Y., Martin, M. E., Brock, H. W., Roeder, R. G., and Hess, J. L. (2005) *Proc. Natl. Acad. Sci. U.S.A.* **102,** 14765–14770
32. Milne, T. A., Briggs, S. D., Brock, H. W., Martin, M. E., Gibbs, D., Allis, C. D., and Hess, J. L. (2002) *Mol. Cell* **10,** 1107–1117
33. Yu, B. D., Hess, J. L., Horning, S. E., Brown, G. A., and Korsmeyer, S. J. (1995) *Nature* **378,** 505–508
34. Terranova, R., Agherbi, H., Boned, A., Meresse, S., and Djabali, M. (2006) *Proc. Natl. Acad. Sci. U.S.A.* **103,** 6629–6634
35. Cheng, X., and Zhang, X. (2007) *Mutat. Res.* **618,** 102–115
36. Qian, C., Wang, X., Manzur, K., Sachchidanand, Farooq, A., Zeng, L., Wang, R., and Zhou, M. M. (2006) *J. Mol. Biol.* **359,** 86–96
37. Trievel, R. C., Flynn, E. M., Houtz, R. L., and Hurley, J. H. (2003) *Nat. Struct. Biol.* **10,** 545–552
38. Xiao, B., Jing, C., Kelly, G., Walker, P. A., Muskett, F. W., Frenkiel, T. A., Martin, S. R., Sarma, K., Reinberg, D., Gamblin, S. J., and Wilson, J. R. (2005) *Genes Dev.* **19,** 1444–1454
39. Xiao, B., Jing, C., Wilson, J. R., Walker, P. A., Vasisht, N., Kelly, G., Howell, S., Taylor, I. A., Blackburn, G. M., and Gamblin, S. J. (2003) *Nature* **421,** 652–656
40. Zhang, X., Yang, Z., Khan, S. I., Horton, J. R., Tamaru, H., Selker, E. U., and Cheng, X. (2003) *Mol. Cell* **12,** 177–185
41. Rice, J. C., Briggs, S. D., Ueberheide, B., Barber, C. M., Shabanowitz, J., Hunt, D. F., Shinkai, Y., and Allis, C. D. (2003) *Mol. Cell* **12,** 1591–1598
42. Couture, J. F., Collazo, E., Brunzelle, J. S., and Trievel, R. C. (2005) *Genes Dev.* **19,** 1455–1465
43. Collins, R. E., Tachibana, M., Tamaru, H., Smith, K. M., Jia, D., Zhang, X., Selker, E. U., Shinkai, Y., and Cheng, X. (2005) *J. Biol. Chem.* **280,** 5563–5570
44. Patel, A., Dharmarajan, V., and Cosgrove, M. S. (2008) *J. Biol. Chem.* **283,** 32158–32161
45. Patel, A., Vought, V. E., Dharmarajan, V., and Cosgrove, M. S. (2008) *J. Biol. Chem.* **283,** 32162–32175
46. Sheffield, P., Garrard, S., and Derewenda, Z. (1999) *Protein Expr. Purif* **15,** 34–39
47. Schuck, P. (2000) *Biophys. J.* **78,** 1606–1619
48. Schuck, P. (2005) in *Analytical Ultracentrifugation: Techniques and Methods* (Scott, D. J., Harding, S. E., and Rowe, A. J. eds.) pp. 26–49, Royal Society of Chemistry, Cambridge, UK
49. Dam, J., Velikovsky, C. A., Mariuzza, R. A., Urbanke, C., and Schuck, P. (2005) *Biophys. J.* **89,** 619–634
50. Laue, T. M., Shah, B. D., Ridgeway, T. M., and Pelletier, S. L. (1992) in *Analytical Ultracentrifugation in Biochemistry and Polymer Science* (Harding, S., Rowe, A., and Horton, J., eds) pp. 19–125, Royal Society of Chemistry, Cambridge, UK
51. Gross, J. W., Hegeman, A. D., Vestling, M. M., and Frey, P. A. (2000) *Biochemistry* **39,** 13633–13640
52. Houston, C. T., Taylor, W. P., Widlanski, T. S., and Reilly, J. P. (2000) *Anal Chem.* **72,** 3311–3319
53. Fersht, A. (1999) *Sturcture and Mechanism in Protein Science*, pp. 143–146, W.H. Freeman and Company, New York
54. Kuzmic, P. (1996) *Anal. Biochem.* **237,** 260–273
55. Kohlmaier, A., Savarese, F., Lachner, M., Martens, J., Jenuwein, T., and Wutz, A. (2004) *PLoS Biol.* **2,** E171
56. Song, J. J., and Kingston, R. E. (2008) *J. Biol. Chem.* **283,** 35258–35264
57. Min, J., Feng, Q., Li, Z., Zhang, Y., and Xu, R. M. (2003) *Cell* **112,** 711–723
58. Southall, S. M., Wong, P. S., Odho, Z., Roe, S. M., and Wilson, J. R. (2009) *Mol. Cell* **33,** 181–191
59. Wilson, J. R., Jing, C., Walker, P. A., Martin, S. R., Howell, S. A., Blackburn, G. M., Gamblin, S. J., and Xiao, B. (2002) *Cell* **111,** 105–115
60. Trievel, R. C., Beach, B. M., Dirk, L. M., Houtz, R. L., and Hurley, J. H. (2002) *Cell* **111,** 91–103
61. Rea, S., Eisenhaber, F., O'Carroll, D., Strahl, B. D., Sun, Z. W., Schmid, M., Opravil, S., Mechtler, K., Ponting, C. P., Allis, C. D., and Jenuwein, T. (2000) *Nature* **406,** 593–599
62. Zhang, X., Tamaru, H., Khan, S. I., Horton, J. R., Keefe, L. J., Selker, E. U., and Cheng, X. (2002) *Cell* **111,** 117–127
63. Manzur, K. L., Farooq, A., Zeng, L., Plotnikova, O., Koch, A. W., Sachchidanand, and Zhou, M. M. (2003) *Nat. Struct. Biol.* **10,** 187–196
64. Dirk, L. M., Flynn, E. M., Dietzel, K., Couture, J. F., Trievel, R. C., and Houtz, R. L. (2007) *Biochemistry* **46,** 3905–3915